JASA ARTICLE

Incipient tip vortex cavitation localization using block-sparse compressive sensing

Minseuk Park,[1] Yongsung Park,[1,a)] Keunhwa Lee,[2] and Woojae Seong[1,b)]
[1]*Department of Naval Architecture and Ocean Engineering, Seoul National University, Seoul, 08826, Republic of Korea*
[2]*Department of Defense Systems Engineering, Sejong University, Seoul, 05006, Republic of Korea*

ABSTRACT:
Noise induced by incipient-propeller tip vortex cavitation (TVC) has a few sources near the propeller tips, which radiate a broadband signal. This article describes a compressive sensing (CS)-based TVC localization technique for coherent multiple-frequency processing, which jointly processes the measured data at multiple frequencies. Block-sparse CS, which groups several single-frequency measurements into blocks, is adopted for coherent multiple-frequency processing. The coherent multiple-frequency processing improves localization performance over that of single-frequency processing. Unlike single-frequency processing using conventional CS, which combines independent single-frequency measurement treatments by averaging, coherent multiple-frequency processing produces accurate localization without requiring a sufficient number of treated frequencies, long-time-sampled data with a time-invariant signal assumption, or even a single cavitation event. The approach is demonstrated on experimental data from a transducer source experiment and a cavitation source experiment. © *2020 Acoustical Society of America*.
https://doi.org/10.1121/10.0001265
(Received 14 November 2019; revised 21 April 2020; accepted 29 April 2020; published online 13 May 2020)
[Editor: Jianlong Li] Pages: 3454–3464

I. INTRODUCTION

Marine propeller cavitation is a dominant noise source phenomenon;[1] thus, it is essential to infer its inception and, possibly, its precise location. Cavitation is of a broadband nature, and previous studies to detect and localize the source of cavitation noise based on the matched-field processing (MFP) method[2] or compressive sensing (CS) method[3] adopted frequency-domain broadband approaches, producing reasonable localization results. The CS-based method[4] showed better localization performance than that of the MFP-based methods.[5–7] However, the CS-based method is not robust to noise compared with the MFP-based method. The aim of this study is to provide a propeller cavitation localization method based on CS that takes advantage of the robustness of the broadband approach to noise and the high-resolution capability of the CS-based method. For this purpose, the block-sparse CS[8–11] technique is adopted, which enables the joint retrieval of multi-frequency components.

Microbubbles incepted by a propeller tip vortex line radiate a short impulse signal during the processes of growth, split, and collapse, which is called tip vortex cavitation (TVC).[1] When the bubbles grow large enough, vortex cavitation can be detected and localized by optical observation. However, optical observation is unavailable when optical access is not allowed or when bubbles are too small to be optically observed. Generally, in the incipient stage of TVC, incepted bubbles are small and invisible to the bare eye; thus, the optical approach is not an appropriate method. More practically, acoustical techniques, implemented either in the time domain[12,13] or frequency domain,[4–7,14,15] can be used to detect and localize the cavitation noise source.

In the time domain, the time difference of arrival (TDOA)-based method is a popular strategy for source localization. The TDOA-based method achieves source localization without computational complexity. However, an accurate estimate of the arrival time is difficult in the presence of the multi-path effect. Generally, in the cavitation tunnel test, the received signal is distorted owing to multi-reflection and noisy environments. The separation of a multi-path signal is sometimes problematic when the received signal waveform is distorted. To localize the vortex cavitation, Chang and Dowling[12] used the TDOA-based method and presented the acoustical localization results. However, they suffered from the effects of reverberation, and additional signal processing had to be used[12,13] to obtain the direct-path signal.

One possible way to mitigate the multi-path effect is to implement source localization in the frequency domain. When the waveform is distorted owing to the multi-path effect, frequency-domain measurement data can be alternatively utilized for source localization. In the case of TVC localization, the MFP-based method using single-frequency measurement data showed that accurate localization can be achieved despite the presence of the multi-path effect.[6] However, single-frequency measurement data still include a frequency interference pattern, reverberation, and background noise, all of which

[a)]Also at: Scripps Institution of Oceanography, University of California San Diego, La Jolla, CA 92093-0238, USA.
[b)]Also at: Research Institute of Marine System Engineering, Seoul National University, Seoul, 08826, Republic of Korea. Electronic mail: wseong@snu.ac.kr, ORCID: 0000-0002-5393-7097.

 0001-4966/2020/147(5)/3454/11/$30.00

hinder accurate localization. Moreover, the single-frequency approach may not be effective under very low signal-to-noise ratio (SNR) conditions. These hindrances can be alleviated by using multi-frequency measurement data.[5–7] Because the received signal at a single frequency includes frequency-dependent information, such as ambiguity surface patterns[2] or environmental characteristics, combining the frequency-dependent information leads to the minimization of unwanted information. There are many different ways to combine frequency-dependent information across frequencies, which can be categorized based on the coherence of the processing method. Incoherent multiple-frequency processing considers each aspect of frequency-dependent information independently of each other. Thus, the information for each frequency is processed individually and combined by direct averaging across frequencies. In contrast, coherent multiple-frequency processing considers each frequency-dependent piece of information cohesively.

The MFP-based method simulates a replica (modeled pressure field induced by a potential noise source) and compares the replica against the measured pressure field of a single frequency at a certain location. This process is performed over multiple frequencies of interest. Then, by exploiting the incoherent multiple-frequency processing, the similarity values are mathematically averaged over frequencies, and the estimation of potential noise source is reached. In the case of TVC noise source localization, Kim *et al.*[6] and Park *et al.*[7] utilized incoherent broadband MFP and showed successful localization results. Because TVC transmits broadband noise, the similarities between the replica and measured pressure field can be compared over multiple frequencies of interest. Despite the fact that each ambiguity surface at a single frequency includes frequency-dependent patterns and sidepeaks that hinder accurate localization, the averaged ambiguity surface effectively mitigates these hindrances. As a result, accurate source localizations were achieved using incoherent broadband MFP.[6,7]

CS is a signal reconstruction technique[3] applicable to sufficiently sparse signals with less measurement data and has shown that it can be applied to the underlying acoustic models which have sparse representations in the basis, such as beamforming,[16–18] geo-acoustic inversion,[19] near-field acoustic holography,[20–22] and underwater source localization.[23] Particularly, Xenaki *et al.*[18] utilized CS for difference of arrival (DOA) reconstruction to overcome the resolution limit of conventional beamforming and showed that the received plane wave signals can be distinguished at high resolution.

Motivated by the CS-based beamforming method,[16,18] Choo and Seong[4] extended the CS technique to the three-dimensional (3D)-spherical beamforming problem using incoherent multiple-frequency processing. Because TVC noise sources can be modeled as few monopole-type broadband sources,[1,6,14] the received signals were approximated as the superposition of the spherical waves induced by potential noise sources. Then, to estimate the locations of the potential noise sources, a sparse reconstruction framework was proposed, assuming that the numerous potential sources are evenly distributed near the propeller region, and sparse reconstruction was performed for all potential sources. Exploiting incoherent multiple-frequency processing, the reconstruction process was conducted at each frequency, and the reconstructed potential sources were averaged across frequencies. In this manner, sparse components were shown to be evident in the averaged solution, which indicates the real source positions.

The CS-based method showed enhanced performance with respect to resolution compared with the MFP-based method. Furthermore, the sparse reconstruction framework offers the additional advantage of not requiring the number of potential noise sources used for localization. When using the MFP-based method, the accuracy of localization is reliant on selecting how many potential noise sources should be used.[14] On the contrary, the CS-based method looks for the sparsest solution; thus, it is not necessary to consider how many potential sources there should be.

Despite the performance improvement in resolution, there are still problems that need to be resolved using the CS-based method. First, the CS-based method[4] does not appear to be robust to noise compared with the MFP-based method,[6] requiring higher SNR for stable reconstruction. However, the time duration of the acoustic signals from cavitation was short, approximately 15 ms long, such that sufficient SNR could not be obtained from a cavitation event. Thus, the CS-based method can be applied only to the long-time-sampled data from several cavitation events. Second, the CS-based method shows a high-resolution localization result but only reveals one dominant source location. In other words, the CS-based method has no capacity to distinguish separate noise sources.

To overcome these shortcomings, we propose an incipient TVC localization method that considers the multiple frequency components jointly. The method assumes that if the preassumed positions (grids) of the potential sources coincide with the true source positions, only the multiple frequency components associated with the corresponding positions would have non-zero elements. Thus, it can be naturally inferred that these multi-frequency components share a spatially common sparse representation and are spectrally grouped together. Exploiting the common sparsity profile assumption, we provide a signal model that can process the multiple frequency components simultaneously and a reconstruction scheme to promote the common sparsity profile. Here, we refer to this joint multiple frequency handling as "coherent multiple-frequency processing." The coherent multiple-frequency processing can provide enhanced localization performance since it finds common sparse representations across different frequency ranges.

To promote the common sparsity profile, we utilize block-sparse CS technique[8] for the reconstruction scheme. If non-zero entries of solution occur only in several partitioned blocks (i.e., the solution has sparse non-zero blocks), such signals are termed as block-sparse. And block-sparse CS technique provides better reconstruction properties than

conventional CS technique when treating the block-sparse signal.[8] It has been shown that recovery performance can be significantly improved using block-sparse CS in the acoustic signal processing problems. For example, in a multiple measurement vector (MMV), problem non-zero elements of every column are temporally correlated under the stationary source assumption. Hence, the solution has a small number of nonzero rows (i.e., the solution is row block-sparse), so that localization performance can be enhanced by promoting spatio-temporal common sparsity.[10,24–26] Another interesting application of block-sparse CS is sparse regularization approach.[27] In practical applications, many acoustic problems are not sparse but clustered in a predefined basis, and there is no prior knowledge of how block partitions lie in the solution. In this case, sparse regularization approach can be a useful tool that promotes the block-sparsity of the solution, and reconstruction performance can be enhanced compared to conventional CS approach.[28–30] Recently, a sparse Bayesian learning (SBL) framework[31] has been applied to the joint sparse problems. The SBL framework provides a probabilistic description between the sparse signal and given measured data, and can be extendedly applied to the block-sparse problem. In many applications (e.g., MMV[32,33] and clustered sparse signal[34] problems), the SBL framework has been effectively used to reconstruct the block-sparse signals by enforcing a common sparsity profile. In this paper, block-sparse CS technique was applied to enforce a common sparsity profile of broadband sources. Because the multiple frequency components associated with the corresponding positions have non-zero elements, while all others have zero elements, non-zero components occur only in clusters (i.e., this signal is block-sparse) and can be reconstructed using block-sparse CS. The reconstruction scheme promotes the common sparsity profile, and thus better localization performance can be achieved compared to the conventional CS approach.

One contribution of our study is the use of coherent multiple-frequency processing, which provides a simultaneous and accurate reconstruction scheme for localizing the broadband sources. For each frequency, complex amplitudes of a broadband source are represented by different dictionaries but share the common spatial grid. To promote this spatially common sparsity profile, we provide a block-diagonal matrix system that makes all of the multiple frequency components be vectorized and the spatially joint components be partitioned as a block. Then, we reconstruct complex amplitudes of multi-frequencies simultaneously exploiting block-sparse CS. Adapting this joint sparse constraint to the reconstruction process, coherent multiple-frequency processing achieves improved accuracy compared with incoherent multiple-frequency processing.

Another contribution is that the proposed method provides high-resolution capability to distinguish separate sources in proximity. Given closely located sources, a low-resolution model (i.e., MFP[6] and incoherent multiple-frequency processing with CS[4]) localizes one dominant source around the true sources but cannot distinguish each source separately. However, the present model achieves high-resolution ability and estimates closely located TVC noise sources at locations identified visually, even with short time length signal.

In Sec. II, we describe coherent multiple-frequency processing using block-sparse CS model to localize the TVC noise source. Section III provides some experimental results to show the performance of the proposed approach, and the performance is compared against that of the conventional CS approach. Finally, Sec. IV provides the conclusion and contributions of the study.

II. BLOCK-SPARSE CS FOR INCIPIENT TVC LOCALIZATION

A. System framework for incipient TVC localization

Incipient TVC is cavitation observed in the vicinity of the propeller tips, more specifically, at the top center of the propeller. The noise source by TVC transmits a monopole-type spherical waveform in all directions and has a broadband frequency spectrum.[12,13,35,36] In the cavitation tunnel, the noise measured at the hydrophones contains multiple paths components, including the direct path and other paths reflected by tunnel walls.[6] In the experiment, the noise source signal that corresponds to the direct path is dominant over the others.[6] Considering a single frequency f monopole source transmission, the received signal through the direct path at the mth hydrophone $y_m^{(f)}$ can be derived as

$$y_m^{(f)} = \frac{e^{-j(2\pi f/c)r_m}}{4\pi r_m} x^{(f)} + n_m^{(f)}, \tag{1}$$

where $y_m^{(f)}$ is the measured sound pressure, c is the water sound speed (here, we use 1502 m/s), r_m is the distance from the cavitation noise source to the mth hydrophone, $x^{(f)}$ is a complex amplitude which has magnitude and initial phase of the cavitation noise, and $n_m^{(f)}$ is the error that involves electric noise, experimental error, or mismatch between actual phenomena and modeling.

In the localization problem, the search space is discretized by potential noise source locations, and the objective is to find the actual locations of the (usually few) noise sources among the assumed potential locations. Let $\mathbf{x}^{(f)} \in \mathbb{C}^N$ be a (sparse) unknown vector we aim to reconstruct, where N is the number of discretized potential locations of noise sources.

The measurement data at the mth hydrophone Eq. (1), which is the superposition of spherical waves from N potential sources, can be expressed using potential noise sources $\mathbf{x}^{(f)}$,

$$y_m^{(f)} = \sum_{n=1}^{N} \frac{e^{-j(2\pi f/c)r_{m,n}}}{4\pi r_{m,n}} x_n^{(f)} + n_m^{(f)}, \tag{2}$$

where $r_{m,n}$ is the distance from the mth hydrophone to the nth potential noise source, and the unknown vector $\mathbf{x}^{(f)}$ is

https://doi.org/10.1121/10.0001265

composed of N complex amplitudes. Note that a fine resolution localization performance is desired; thus, $M \ll N$.

Then, the relationship between M hydrophones and N potential noise sources can be expressed as

$$\mathbf{y}^{(f)} = \mathbf{A}^{(f)}\mathbf{x}^{(f)} + \mathbf{n}^{(f)}, \tag{3}$$

where $\mathbf{y}^{(f)}$ is the measurement vector at M hydrophones $\mathbf{y}^{(f)} \in \mathbb{C}^M$, and the (m, n)th entry of the matrix $\mathbf{A}^{(f)} \in \mathbb{C}^{M\times N}$ is given by

$$A_{m,n}^{(f)} = \frac{e^{-j(2\pi f/c)r_{m,n}}}{4\pi r_{m,n}}. \tag{4}$$

The nth column of the matrix $\mathbf{A}^{(f)}$, $\mathbf{a}_n^{(f)}$, is the replica vector, which reflects the transmission from the nth potential noise source to the hydrophones.

In the localization method, let the incipient TVC noise comprise K-sparse sources; then, the incipient TVC localization problem is to find the actual locations of K noise sources among the assumed N locations ($K \ll N$). Equivalently, it is to find a linear combination of K-sparse bases (columns) out of *a priori* N bases in the sensing matrix $\mathbf{A}^{(f)}$.

B. Incoherent multiple-frequency localization with CS

As the noise source from the incipient TVC has a broadband frequency spectrum, we can utilize multiple-frequency measurements. Multiple-frequency processing exploring all the multiple-frequency measurements is an intuitive way to improve the localization performance.

For single-frequency processing, the incipient TVC localization problem is to recover a linear combination of K-sparse bases (columns) in *a priori* N bases of the sensing matrix $\mathbf{A}^{(f)}$, Eq. (3). Equivalently, it is to recover a sparse solution $\mathbf{x}$. CS recovers a sparse solution by minimizing the sparsity-enforcing norm (l_1-norm), *i.e.*, $\|\mathbf{x}\|_1 = \sum_{n=1}^{N} |x_n|$.

The incipient TVC localization problem using a single-frequency CS can be solved by the following the l_1-norm minimization problem:

$$\min_{\hat{\mathbf{x}}^{(f)}\in\mathbb{C}^N} \|\hat{\mathbf{x}}^{(f)}\|_1 \ \text{ subject to } \ \|\hat{\mathbf{y}}^{(f)} - \hat{\mathbf{A}}^{(f)}\hat{\mathbf{x}}^{(f)}\|_2 \le \hat{\epsilon}, \tag{5}$$

where $\hat{\mathbf{y}}^{(f)}$ and $\hat{\mathbf{a}}_n^{(f)}$ are normalized versions of $\mathbf{y}^{(f)}$ and $\mathbf{a}_n^{(f)}$, *i.e.*, $\hat{\mathbf{y}}^{(f)} = \mathbf{y}^{(f)}/\|\mathbf{y}^{(f)}\|_2$ and $\hat{\mathbf{a}}_n^{(f)} = \mathbf{a}_n^{(f)}/\|\mathbf{a}_n^{(f)}\|_2$. The nth entry of $\hat{\mathbf{x}}^{(f)}$ is $(\|\mathbf{a}_n\|_2/\|\mathbf{y}\|_2)x_n$. The normalization causes the candidate bases in $\mathbf{A}$ to have the same Euclidean norm, such that it prevents the bias induced by different distances $r_{m,n}$.[4,8] $\hat{\epsilon}$ is the error floor that controls the error between measurements and the obtained results with respect to the l_2-norm. With large $\hat{\epsilon}$, we can obtain a very sparse solution permitting a large amount of error with poor data fit. With small $\hat{\epsilon}$, the resulting solution follows the measured data closely with overfitting, and it is not likely to have a sparse representation.

To utilize multiple frequencies of incipient TVC, incoherent multiple-frequency processing with CS can be used where single-frequency processing solutions across the multiple frequencies are applied individually and provide a more stable estimation. Incoherent multiple-frequency processing with CS involves obtaining a sparse solution at each single frequency, Eq. (5), and taking an average over the obtained sparse solutions,

$$\hat{\mathbf{x}}_{\text{incoh}} = \frac{1}{L}\sum_{l=1}^{L} |\hat{\mathbf{x}}^{(f_l)}|, \tag{6}$$

where f_l is the lth frequency for L frequencies in the TVC frequency spectrum. Then estimated amplitude of nth potential source which averaged across frequencies can be written as

$$s_{n,incoh} = \hat{x}_{n,\text{incoh}}, \tag{7}$$

where $\hat{x}_{n,\text{incoh}}$ stands for nth entry of solution $\hat{\mathbf{x}}_{\text{incoh}}$ in Eq. (6). Therefore, source locations can be estimated by seeking for the non-zero $s_{n,incoh}$ value.

Note that the corresponding solution $\hat{\mathbf{x}}$ becomes less sparse if the single-frequency solutions $\hat{\mathbf{x}}^{(f_l)}$ do not share the non-zero components at the same locations. To take advantage of incoherent multiple-frequency processing, the conditions for single-frequency localization has to be satisfied; that is, high SNR, sufficient length of time-sample data, or sufficient number of frequencies is required.

C. Coherent multiple-frequency localization with block-sparse CS

The multiple-frequency CS-based incipient TVC localization problem can be solved using coherent multiple-frequency processing with CS. To better understand the coherent multiple-frequency CS structure, we provide an explanation of the MMV problem.[10,24,25] The MMV problem recovers the joint sparse source signals from a set of L measurement vectors. These vectors share the same non-zero support, which promotes spatial sparsity; thus, the signal can be reconstructed with high resolution. With L measurement vectors, this MMV model can be expressed as

$$\mathbf{Y} = \mathbf{A}\mathbf{X} + \mathbf{N}, \tag{8}$$

where the MMVs $\mathbf{Y} \in \mathbb{C}^{M\times L}$, the sensing matrix $\mathbf{A} \in \mathbb{C}^{M\times N}$, and the N potential vectors $\mathbf{X} \in \mathbb{C}^{N\times L}$. For stationary sources, this approach can be utilized to enhance the localization performance. However, since vortex cavitation is a short-duration noise source of broadband, the MMV model is not appropriate for the localization method. Instead of the MMV problem, we introduce the multiple-frequency measurement vector, which promotes spatial sparsity.

Each single-frequency sparse model, Eq. (5), uses a different sensing matrix for each frequency; thus, MMV formation cannot be utilized for the multiple frequency measurement vectors. To use multiple-frequency

measurement vectors, block-sparse CS is utilized to combine the set of the single-frequency sparse models into a block-sparse model, as shown in Fig. 1, i.e., multiple-frequency measurement vectors are combined into a single vector.

With this concept and L frequencies $(f_1, \ldots, f_L)$ in the TVC frequency spectrum, we can extend the normalized version of the sparse measurement model, $\hat{\mathbf{y}}^{(f)} = \hat{\mathbf{A}}^{(f)}\hat{\mathbf{x}}^{(f)}$, as a block-sparse measurement model,

$$\tilde{\mathbf{y}} = \tilde{\mathbf{A}}\tilde{\mathbf{x}} + \tilde{\mathbf{n}}, \tag{9}$$

where multiple-frequency measurement vector $\tilde{\mathbf{y}} \in \mathbb{C}^{ML}$, sensing matrix of block-sparse model $\tilde{\mathbf{A}} \in \mathbb{C}^{ML \times NL}$ (M, number of receivers; N, number of potential sources; L, number of frequencies). Multiple-frequency measurement vector $\tilde{\mathbf{y}}$ and block-sparse vector $\tilde{\mathbf{x}} \in \mathbb{C}^{NL}$ take the forms

$$\begin{aligned}\tilde{\mathbf{y}} &= [\tilde{\mathbf{y}}_1^{\text{block}}; \cdots; \tilde{\mathbf{y}}_M^{\text{block}}] \\ &= [\underbrace{\tilde{y}_1^{(f_1)}, \ldots, \tilde{y}_1^{(f_L)}}_{\tilde{\mathbf{y}}_1^{\text{block}},} \ldots, \underbrace{\tilde{y}_M^{(f_1)}, \ldots, \tilde{y}_M^{(f_L)}}_{\tilde{\mathbf{y}}_M^{\text{block}}}]^{\mathsf{T}},\end{aligned} \tag{10}$$

$$\begin{aligned}\tilde{\mathbf{x}} &= [\tilde{\mathbf{x}}_1^{\text{block}}; \cdots; \tilde{\mathbf{x}}_N^{\text{block}}] \\ &= [\underbrace{\tilde{x}_1^{(f_1)}, \ldots, \tilde{x}_1^{(f_L)}}_{\tilde{\mathbf{x}}_1^{\text{block}},} \ldots, \underbrace{\tilde{x}_N^{(f_1)}, \ldots, \tilde{x}_N^{(f_L)}}_{\tilde{\mathbf{x}}_N^{\text{block}}}]^{\mathsf{T}},\end{aligned} \tag{11}$$

and

$$\tilde{\mathbf{A}} = \begin{bmatrix} \tilde{\mathbf{A}}_{1,1}^{\text{block}} & \cdots & \tilde{\mathbf{A}}_{1,N}^{\text{block}} \\ \vdots & \ddots & \vdots \\ \tilde{\mathbf{A}}_{M,1}^{\text{block}} & \cdots & \tilde{\mathbf{A}}_{M,N}^{\text{block}} \end{bmatrix}, \tag{12}$$

where $\tilde{\mathbf{A}}_{m,n}^{\text{block}}$ is the (m, n)th partition of the matrix $\tilde{\mathbf{A}}$,

$$\begin{aligned}\tilde{\mathbf{A}}_{m,n}^{\text{block}} &= \text{diag}(\hat{a}_{m,n}^{(f_1)}, \ldots, \hat{a}_{m,n}^{(f_L)}) \\ &= \begin{bmatrix} \hat{a}_{m,n}^{(f_1)} & 0 & \cdots & 0 \\ 0 & \hat{a}_{m,n}^{(f_2)} & \cdots & 0 \\ \vdots & \vdots & \ddots & \vdots \\ 0 & 0 & \cdots & \hat{a}_{m,n}^{(f_L)} \end{bmatrix},\end{aligned} \tag{13}$$

and $\hat{a}_{m,n}^{(f_l)}$ is the (m, n)th entry of the matrix $\hat{\mathbf{A}}^{(f_l)}$ in Eq. (5). Note that the solution $\tilde{\mathbf{x}}$ is blockwise sparse.

In Eq. (11), we can infer that the unknown parameters to be solved have been increased from N to NL. This means that if there are K-sparse sources, we should solve KL sparse problem. Fortunately, a few sources that have broadband characteristics can be expressed as block-sparse $\tilde{\mathbf{x}}$; thus, we can utilize the block-sparse CS to solve the more optimal K-sparse problem than the KL-sparse problem. As $\tilde{\mathbf{x}}$ is K-block-sparse, the localization problem is to find a combination of K-sparse column-blocks in *a priori* N column-blocks of the block-sparse sensing matrix $\tilde{\mathbf{A}}$.

To solve the K-block-sparse system, we use an l_2/l_1-norm minimization technique[8] to find the nonzero blocks. Just as the l_1-norm minimization technique[3] used in conventional CS, l_2/l_1-norm minimization technique minimizes the sum of the l_2-norm of the blocks.

Then, the incipient TVC localization with block-sparse CS is solved using the following formulation:

$$\min_{\tilde{\mathbf{x}} \in \mathbb{C}^{NL}} \sum_{n=1}^{N} \|\tilde{\mathbf{x}}_n^{\text{block}}\|_2 \text{ subject to } \|\tilde{\mathbf{y}} - \tilde{\mathbf{A}}\tilde{\mathbf{x}}\|_2 \le \tilde{\epsilon}, \tag{14}$$

where $\tilde{\mathbf{x}}_n^{\text{block}} = [\tilde{x}_n^{(f_1)}, \ldots, \tilde{x}_n^{(f_L)}]^{\mathsf{T}}$ and $\tilde{\epsilon}$ is the error floor, in which the role is similar to that of $\hat{\epsilon}$ in Eq. (5). Note that sparsity is imposed on the l_2-norm of the blocks of vector $\tilde{\mathbf{x}}$.

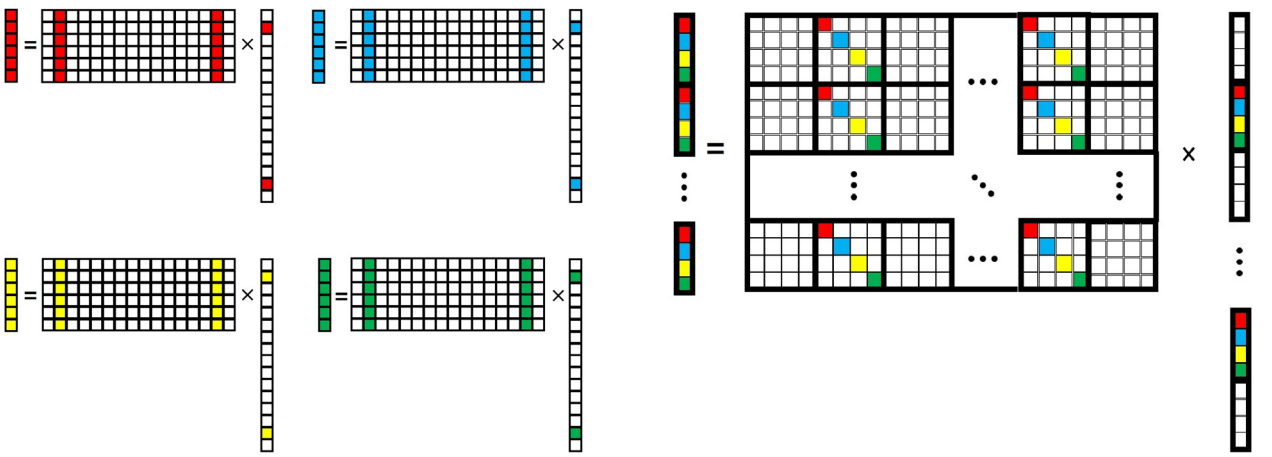

(a) Incoherent processing (b) Coherent processing

FIG. 1. (Color online) (a) Conventional CS model with MMV. Each color indicates temporal difference and the non-zero components in the measurement vectors share the same dictionaries because they are temporally correlated (sparsity level is two). (b) Block-sparse CS model for coherent multiple-frequency processing. Each color indicates frequency difference and the non-zero components in the measurement vector correspond to the different dictionaries because they are uncorrelated (block-sparsity level is two).

https://doi.org/10.1121/10.0001265

Referring to Eqs. (5) and (14), the dimension of unknown vector to be reconstructed have been increased $\mathbf{x}^{(f)} \in \mathbb{C}^N$ to $\tilde{\mathbf{x}} \in \mathbb{C}^{NL}$, where $\tilde{\mathbf{x}}$ is a block-sparse vector.

We considered the problem of reconstructing a block-sparse vector that represents the broadband acoustic sources. As these sources are sparse and broadband, entries of the block corresponding to real source positions will all be non-zero. Thus, the problem of using block-sparse CS will not increase the sparsity, even though the number of unknown parameters is increased, but rather enhance the sparsity.[8]

To localize the TVC sources, we consider the case of only a few broadband sources, i.e., $\tilde{\mathbf{x}}$ is block-sparse. We assume that the TVC sources are sparse; thus, the spatial candidates (number of potential sources) are not increased compared with the number of incoherent parameters (number of potential sources). This means that the increased number of unknown parameters do not increase the sparsity (i.e., block-sparsity) for this problem. As expressed in Eq. (14), we search for candidates representing the real source signal. Using the block-sparse concept, this means that certain potential sources radiate a broadband signal, rather than a tonal signal, and signal vectors will be reconstructed only with fully filled blocks or fully blank blocks. Therefore, the amplitude of the nth potential source for coherent multiple-frequency processing can be written as

$$s_{n,coh} = ||\tilde{\mathbf{x}}_n^{\text{block}}||_2, \tag{15}$$

where $\tilde{\mathbf{x}}_n^{\text{block}}$ stands for the nth block of solution $\tilde{\mathbf{x}}$ in Eq. (11) and source locations can be estimated by seeking for the non-zero $s_{n,coh}$ value.

III. BLOCK-SPARSE CS FOR INCIPIENT TVC LOCALIZATION

In this section, we apply the block-sparse CS to measurement data from the cavitation tunnel experiments for incipient TVC localization. Two experiments were conducted with a transducer source (known source position) and an incipient TVC noise source. For a localization search grid with potential noise sources, the potential sources are evenly distributed near the true source location at a 0.05 m interval for the transducer source case and a 0.01 m interval for the incipient TVC noise source case. The objective of the transducer source experiment is to validate the block-sparse CS localization algorithm and compare the localization results from coherent multiple-frequency processing to those from incoherent multiple-frequency processing. The objective of the incipient TVC noise source experiment is to demonstrate the high-resolution capabilities and robustness of the block-sparse CS in the incipient TVC localization.

A. Transducer source experiment

The high-resolution performance of block-sparse CS, coherent multiple-frequency processing, is validated with experimental data from cavitation tunnel experiments, and it is compared with conventional CS and incoherent multiple-frequency processing.

The configuration of the transducer source experiment is shown in Fig. 2(a). One transducer source (ITC-1001) with known location information was located in the cavitation tunnel and was transmitting a broadband signal, whose spectrum ranged from 7 to 37 kHz. The data set was collected on $M = 6$ hydrophones (B&K 8103) mounted beneath the upper part of the cavitation tunnel. Here, we set the potential transducer noise sources (the localization search grid) to be evenly distributed near the true source location with a 0.05 m interval over a 3D volume (x axis: −0.5–0.5 m, y axis: −1.4–0 m, z-axis: −1.5–1.5 m), i.e., the number of candidates $N = 37\,149$ ($21 \times 29 \times 61$).

Coherent multiple-frequency processing with block-sparse CS is compared to incoherent multiple-frequency processing with conventional CS,[4] as shown in Fig. 3. Here, we use $L = 10$ frequencies ([7, 10, 13, 16, 19, 22, 25, 28, 31, 34] kHz). We have chosen error floors $\hat{\epsilon}$ [Eq. (5)] and $\tilde{\epsilon}$ [Eq. (14)] for the results to have a sparsity level of three. Coherent multiple-frequency processing estimates the true location of the transducer source with one significant component, but incoherent multiple-frequency processing fails to localize the source.

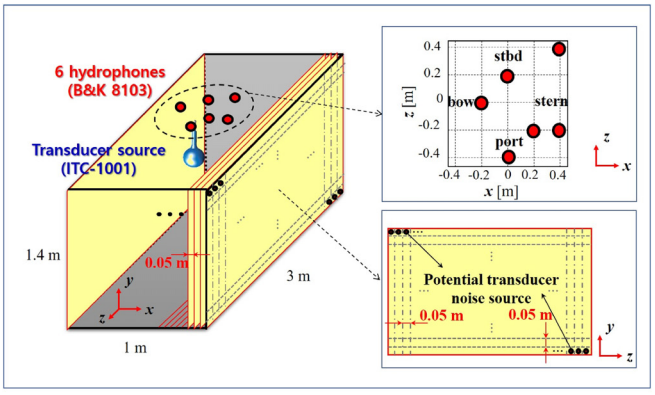

(a) Transducer source experiment

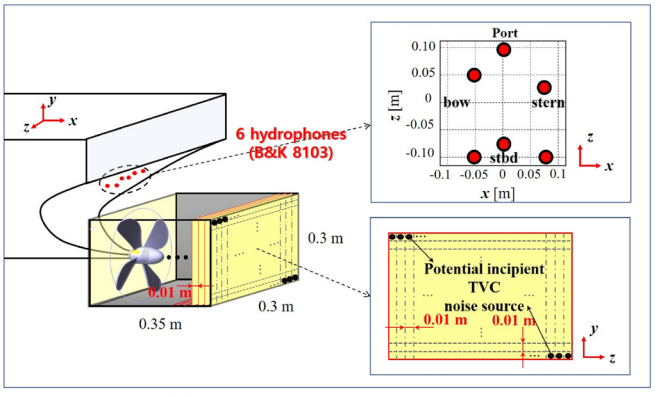

(b) Cavitation source experiment

FIG. 2. (Color online) Schematic plan of hydrophones and potential noise sources (search grid) for (a) the transducer source experiment and (b) the incipient TVC source experiment.

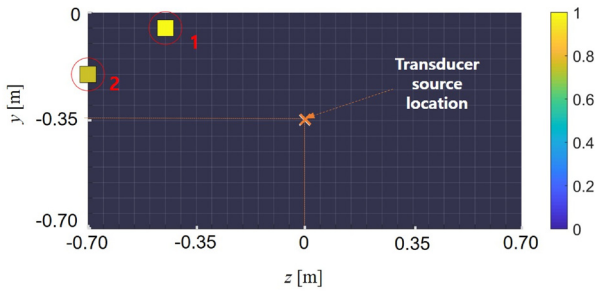

(a) Incoherent multiple-frequency processing

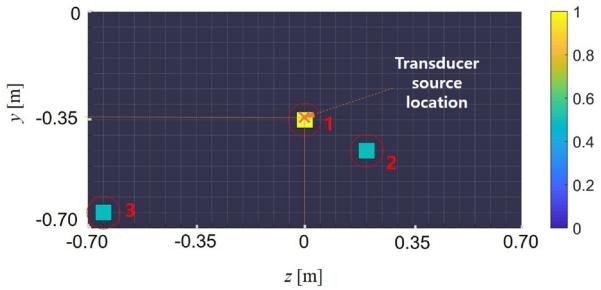

(b) Coherent multiple-frequency processing

FIG. 3. (Color online) Source localization with experimental data for the transducer source, of which location is known, with (a) conventional CS (incoherent multiple-frequency processing) and (b) block-sparse CS (coherent multiple-frequency processing) on the y–z plane at a fixed $x = 0$ m. The three largest source amplitudes [Eqs. (7) and (15)] are plotted and each amplitude are normalized to a maximum amplitude of one.

The localization performance of incoherent multiple-frequency processing can be improved by processing many frequency components, as shown in Fig. 4. The number of processed frequencies varies from $L = 30$ [Fig. 4(b)] to $L = 120$ [Fig. 4(d)] in the 7–37 kHz frequency band. Incoherent multiple-frequency processing with conventional CS requires a sufficient number of meaningful single-frequency processing solutions that localize the true source location. Still, even though a number of frequencies are considered as in Fig. 4(d), the dominant source, which characterizes the overall multiple-frequency pressure field, is not noticeably distinguished from the other candidates without sufficiently high SNR. Note that this localization can be regarded as a 1-sparse problem. However, it is apparent from Figs. 3 and 4 that incoherent multiple-frequency processing cannot provide a stable localization result without sufficiently high SNR and without sufficient measurement information.

B. Incipient TVC noise source experiment

In this section, block-sparse CS for incipient TVC localization is applied to the experimental data from the cavitation tunnel experiment. The configuration of the incipient TVC source experiment is shown in Fig. 2(b). The data set was collected on $M = 6$ hydrophones (B&K 8103) mounted on the hull surface of the model ship above the propeller.

Incipient TVC is observed at the top center of the propeller near the propeller tip, as shown in Fig. 5(a). Noise induced by the incipient TVC is emitted in all directions and

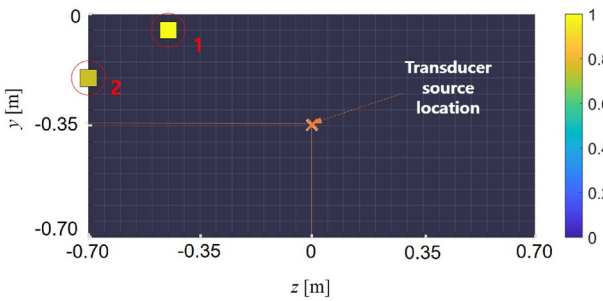

(a) 10 frequencies

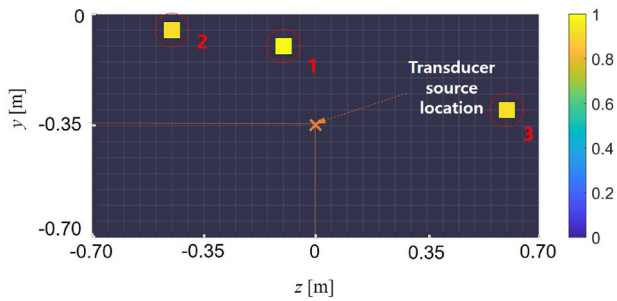

(b) 30 frequencies

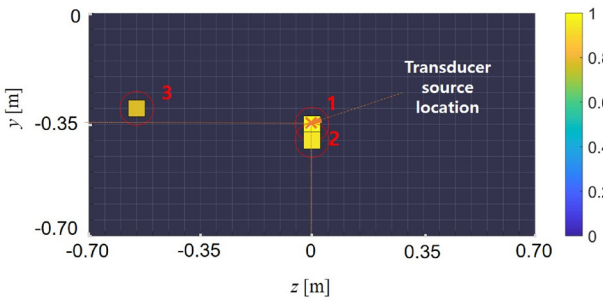

(c) 60 frequencies

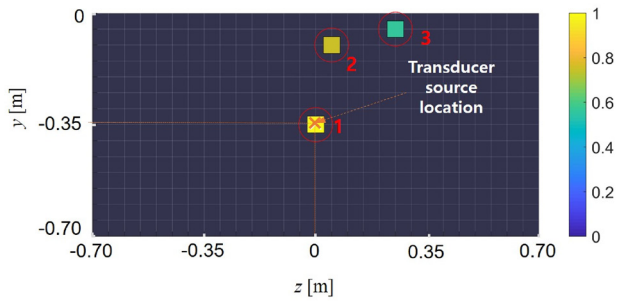

(d) 120 frequencies

FIG. 4. (Color online) Same as Fig. 3, except for incoherent multiple-frequency processing with different numbers of processed frequencies.

https://doi.org/10.1121/10.0001265

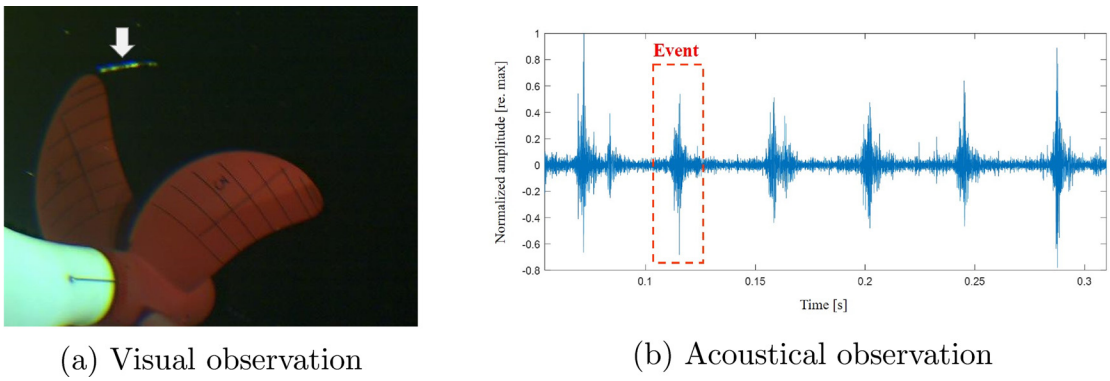

(a) Visual observation (b) Acoustical observation

FIG. 5. (Color online) (a) Visual observation of TVC and (b) measured acoustic data in the incipient TVC stage. The acoustic data in the time domain is bandpass-filtered (20–50 kHz).

can be modeled as a monopole source.[6] The TVC noise has a broadband frequency spectrum,[1] and bandpass-filtered (20–50 kHz) acoustic measurement data in the time domain is shown in Fig. 5(b). Readers are referred to Refs. 4 and 6 for detailed discussions on the experimental configuration.

Here, we set the potential TVC noise sources (the localization search grid) to be evenly distributed near the top center of the propeller with a 0.01 m interval over a 3D volume (x axis: −0.05–0.3 m, y axis: −0.15–0.15 m, z-axis: −0.15–0.15 m), i.e., the number of candidates $N = 34,596$ ($36 \times 31 \times 31$). We have chosen the error floors $\hat{\epsilon}$ [Eq. (5)] and $\tilde{\epsilon}$ [Eq. (14)] for the results to have a sparsity level of three (here, we manually selected error floor for 0.3). Then, we have solved Eqs. (5) and (14) by utilizing the CVX toolbox.[37]

Table I shows the numerical results for the coherent multiple-frequency processing and the incoherent multiple-frequency processing. To examine the localization performance for multiple noise sources, localization errors between simulated sources and estimated sources are analyzed comparing the coherent multiple-frequency processing with the incoherent multiple-frequency processing. We generated randomly distributed (on the search grids) monopole sources with random amplitudes (normalized between 0.5 and 1.0) and random phases ([0–2π]) over selected frequencies ([20 : 2.5 : 50] kHz). The number of generated monopole sources are selected according to the sparsity level (=1–3). Complex Gaussian noise is added to the measurement with a 20 dB signal-to-noise ratio (which is similar to that of the cavitation measurement data) and the rest of the simulation setup is the same as real TVC experimental configuration. Then the localization was conducted for each processing and localization errors were estimated in terms of the number of the sources (=sparsity level) as illustrated in Table I. It is apparent from Table I that coherent multiple-frequency processing is accurate over various sparsity levels (note that spatial grid is evenly distributed with a 0.01 m interval) and localization errors grow as the sparsity level increases. We can infer that coherent multiple-frequency processing has the capability to distinguish spatially separate sources. However, incoherent multiple-frequency processing only works in the case of sparsity level 1. This means that incoherent multiple-frequency processing is not the proper method for the multiple-source localization problem.

Then, the processes are applied to experimental TVC data and coherent multiple-frequency processing with block-sparse CS [Fig. 6(b)] is compared to incoherent multiple-frequency processing with conventional CS[4] [Fig. 6(a)]. As incoherent multiple-frequency processing requires a sufficient number of frequencies to be processed, different numbers of frequencies are considered: $L = 13$ frequencies ([20 : 2.5 : 50] kHz) for coherent multiple-frequency processing and $L = 121$ frequencies ([20 : 0.25 : 50] kHz) for incoherent multiple-frequency processing.

Coherent multiple-frequency processing estimates two locations around the top center of the propeller and at the downstream direction [Fig. 6(b)]. Because the tip vortex line is induced at the back of the propeller, the localization result corresponds to the visual observation [Fig. 5(a)]. In contrast, incoherent multiple-frequency processing fails to estimate a dominant location, and it localizes one near the top of the propeller but with the second largest component [Fig. 6(a)].

Figure 7 shows the distribution of the largest components of the localization results for 200 cavitation events

TABLE I. Mean localization error simulation result in terms of sparsity level. The source numbers are sorted from large to small amplitude (source 1 is the largest one).

	Coherent processing			Incoherent processing		
Case	Source 1	Source 2	Source 3	Source 1	Source 2	Source 3
Sparsity = 1	0.0004 m	—	—	0.0003 m	—	—
Sparsity = 2	0.0019 m	0.0039 m	—	0.1151 m	0.1513 m	—
Sparsity = 3	0.0176 m	0.0203 m	0.0299 m	0.1338 m	0.1674 m	0.1796 m

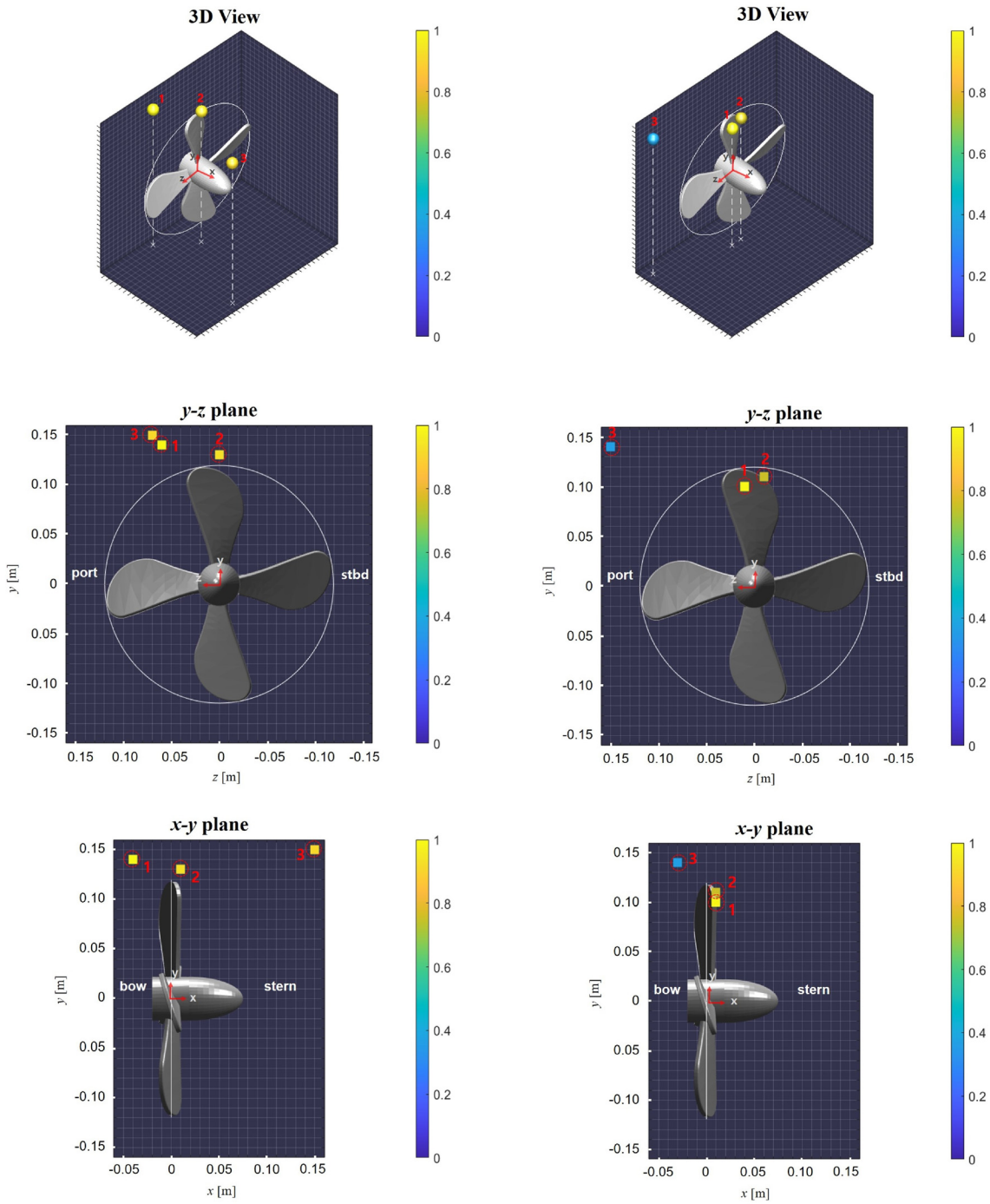

(a) Incoherent multiple-frequency processing (b) Coherent multiple-frequency processing

FIG. 6. (Color online) Source localization with experimental data for the cavitation source with (a) conventional CS (incoherent multiple-frequency processing) and (b) block-sparse CS (coherent multiple-frequency processing). The three largest source amplitudes [Eqs. (7) and (15)] are plotted, and each amplitude is normalized to a maximum amplitude of one.

[Fig. 5(b)]. The localization results are concentrated around the top center of the propeller [Fig. 7(a)] and at the downstream direction [Fig. 7(b)]. Note that the variability of the estimated locations in the x axis is small.

The multiple-frequency data with block-sparse CS reveals that block-sparse CS enables coherent multiple-frequency processing over multiple frequencies and acoustically localizes the TVC noise source in accordance with the visual signature of the TVC.

IV. CONCLUSION

The purpose of this paper is to localize the incipient TVC noise sources via block-sparse CS. CS is applied in the

https://doi.org/10.1121/10.0001265

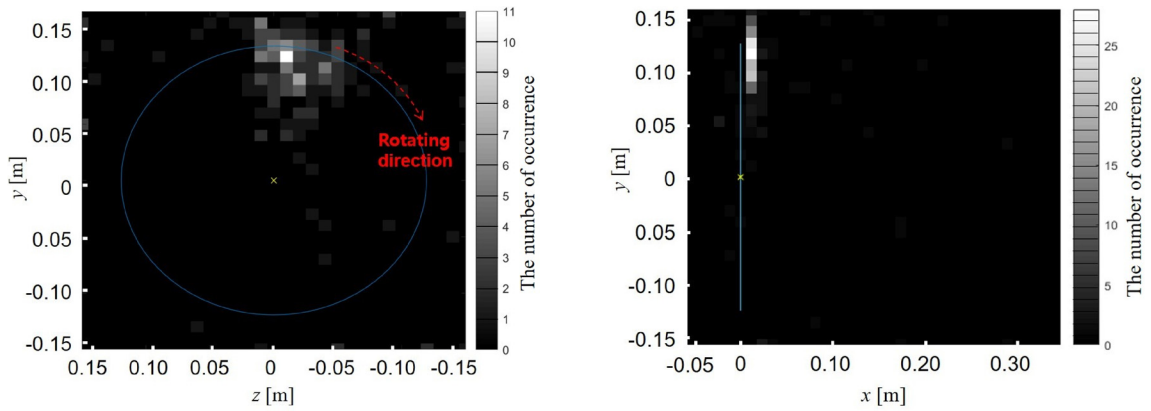

(a) y-z plane (b) x-y plane

FIG. 7. (Color online) Histogram of the locations of the largest estimated sources for 200 cavitation events on (a) the y–z plane at a fixed $x = 0$ m and (b) the x–y plane at a fixed $z = 0$ m.

sparse nature of the TVC noise sources. Given that TVC noise radiates a broadband signal, multiple-frequency processing improves performance in localization over single-frequency processing. For coherent multiple-frequency processing, which jointly considers the measured data at multiple frequencies, block-sparse CS is utilized.

In contrast to incoherent multiple-frequency processing using conventional CS, coherent multiple-frequency processing provides accurate localization results, even with a fewer number of processed frequencies. Also, coherent multiple-frequency processing does not need long-time-sampled data with a time-invariant signal assumption to obtain high resolution in incoherent multiple-frequency processing.

The real data results indicate that the block-sparse CS is capable of localizing the incipient TVC noise sources, and the estimated locations correspond with the visual observations of TVC.

ACKNOWLEDGMENTS

This research was supported by the Agency for Defense Development in Korea under Contract No. UD190005DD, and the National Research Foundation of Korea (NRF) Grant No. 2016R1C1B1011545.

[1]Y. Lecoffre, *Cavitation: Bubble Trackers* (Balkema, Leiden, the Netherlands, 1999), pp. 140–210.
[2]A. Tolstoy, *Matched Field Processing for Underwater Acoustics* (World Scientific Publishing, Singapore, 1993), pp. 91–180.
[3]D. L. Donoho, "Compressed sensing," IEEE Trans. Inf. Theory **52**(4), 1289–1306 (2006).
[4]Y. Choo and W. Seong, "Compressive spherical beamforming for localization of incipient tip vortex cavitation," J. Acoust. Soc. Am. **140**(6), 4085–4090 (2016).
[5]C. Park, H. Seol, K. Kim, and W. Seong, "A study on propeller noise source localization in a cavitation tunnel," Ocean Eng. **36**, 754–762 (2009).
[6]D. Kim, W. Seong, Y. Choo, and J. Lee, "Localization of incipient tip vortex cavitation using ray based matched field inversion method," J. Sound Vib. **354**, 34–46 (2015).
[7]C. Park, G. Kim, Y. Park, K. Lee, and W. Seong, "Noise localization method for model tests in a large cavitation tunnel using a hydrophone array," Remote Sens. **8**(3), 195–218 (2016).
[8]Y. C. Eldar, P. Kuppinger, and H. Bolcskei, "Block-sparse signals: Uncertainty relations and efficient recovery," IEEE Trans. Signal Process. **58**(6), 3042–3054 (2010).
[9]R. G. Baraniuk, V. Cevher, M. F. Duarte, and C. Hegde, "Model-based compressive sensing," IEEE Trans. Inf. Theory **56**(4), 1982–2001 (2010).
[10]J. Tropp, A. C. Gilbert, and M. J. Strauss, "Algorithms for simultaneous sparse approximation. part i: Greedy pursuit," Signal Process. **86**(3), 572–588 (2006).
[11]M. Yuan and Y. Lin, "Model selection and estimation in regression with grouped variables," J. R. Stat. Soc. Ser. B **68**, 49–67 (2006).
[12]N. A. Chang and D. R. Dowling, "Ray-based acoustic localization of cavitation in a highly reverberant environment," J. Acoust. Soc. Am. **125**(5), 3088–3100 (2009).
[13]N. A. Chang and S. L. Ceccio, "The acoustic emissions of cavitation bubbles in stretched vortices," J. Acoust. Soc. Am. **130**(5), 3209–3219 (2011).
[14]K. Lee, J. Lee, D. Kim, K. Kim, and W. Seong, "Propeller sheet cavitation noise source modeling and inversion," J. Sound Vib. **333**(5), 1356–1368 (2014).
[15]D. Kim, K. Lee, and W. Seong, "Non-cavitating propeller noise modeling and inversion," J. Sound Vib. **333**(24), 6424–6437 (2014).
[16]D. Malioutov, M. Cetin, and A. Willsky, "A sparse signal reconstruction perspective for source localization with sensor arrays," IEEE Trans. Signal Process. **53**(8), 3010–3022 (2005).
[17]N. Wagner, Y. C. Eldar, and Z. Friedman, "Compressed beamforming in ultrasound imaging," IEEE Trans. Signal Process. **60**(9), 4643–4657 (2012).
[18]A. Xenakia and P. Gerstoft, "Compressive beamforming," J. Acoust. Soc. Am. **136**(1), 260–271 (2014).
[19]C. Yardim, P. Gerstoft, W. S. Hodgkiss, and J. Traer, "Compressive geoacoustic inversion using ambient noise," J. Acoust. Soc. Am. **135**(3), 1245–1255 (2014).
[20]G. Chardon, L. Daudet, A. Peillot, F. Ollivier, N. Bertin, and R. Gribonval, "Near-field acoustic holography using sparse regularization and compressive sampling principles," J. Acoust. Soc. Am. **132**(3), 1521–1534 (2012).
[21]E. Fernandez-Grande, A. Xenaki, and P. Gerstoft, "A sparse equivalent source method for near-field acoustic holography," J. Acoust. Soc. Am. **141**(1), 532–542 (2017).
[22]C. X. Bi, Y. Liu, L. Xu, and Y. Zhang, "Sound field reconstruction using compressed modal equivalent point source method," J. Acoust. Soc. Am. **141**(1), 73–79 (2017).
[23]P. A. Forero and P. A. Baxley, "Shallow-water sparsity-cognizant source-location mapping," J. Acoust. Soc. Am. **135**(6), 3483–3501 (2014).
[24]P. Gerstoft, A. Xenaki, and C. F. Mecklenbrauker, "Multiple and single snapshot compressive beamforming," J. Acoust. Soc. Am. **138**(4), 2003–2014 (2015).

[25]S. F. Cotter, B. D. Rao, K. Engan, and K. Kreutz-Delgado, "Sparse solutions to linear inverse problems with multiple measurement vectors," IEEE Trans. Signal Process. **53**(7), 2477–2488 (2005).
[26]Y. Park, Y. Choo, and W. Seong, "Multiple snapshot grid free compressive beamforming," J. Acoust. Soc. Am. **143**(6), 3849–3859 (2018).
[27]R. Tibshirani and J. Taylor, "The solution path of the generalized lasso," Ann. Stat. **39**(3), 1335–1371 (2011).
[28]A. Xenaki, E. Fernandez-Grande, and P. Gerstoft, "Block-sparse beamforming for spatially extended sources in a Bayesian formulation," J. Acoust. Soc. Am. **140**(3), 1828–1838 (2016).
[29]E. Fernandez-Grande and L. Daudet, "Compressive acoustic holography with block-sparse regularization," J. Acoust. Soc. Am. **143**, 3737–3746 (2018).
[30]Y. Park, W. Seong, and P. Gerstoft, "Block-sparse two-dimensional off-grid beamforming with arbitrary planar array geometry," J. Acoust. Soc. Am. **147**(4), 2184–2191 (2020).
[31]M. E. Tipping, "Sparse Bayesian learning and the relevance vector machine," J. Mach. Learn. Res. **1**, 211–244 (2001).
[32]D. P. Wipf and B. Rao, "An empirical Bayesian strategy for solving the simultaneous sparse approximation problem," IEEE Trans. Signal Process. **55**(7), 3704–3716 (2007).
[33]P. Gerstoft, C. Mecklenbrauker, A. Xenaki, and S. Nannuru, "Multi-snapshot sparse Bayesian learning for DOA," IEEE Signal Process. Lett. **23**, 1469–1473 (2016).
[34]Z. Zhang and B. Rao, "Sparse signal recovery with temporally correlated source vectors using sparse Bayesian learning," IEEE J. Sel. Topics Signal Process. **5**(5), 912–926 (2011).
[35]J. Choi and G. L. Chahine, "Noise due to extreme bubble deformation near inception of tip vortex cavitation," Phys. Fluids **16**(7), 2411–2418 (2004).
[36]J. Choi and S. L. Ceccio, "Dynamics and noise emission of vortex cavitation bubbles," J. Fluid Mech. **575**, 1–26 (2007).
[37]M. Grant, S. Boyd, and Y. Ye, "CVX: Matlab software for disciplined convex programming, version 2.1," http://cvxr.com/cvx (Last viewed April 11, 2019).